

STRUCTURAL RESPONSE OF A BLAST LOADED FUSELAGE

Adam Dacko, Jacek Toczyski

Warsaw University of Technology
Faculty of Power and Aeronautical Engineering
Nowowiejska Street 24, 00-665 Warszawa
e-mail: adam.dacko@meil.pw.edu.pl, jtozyski@meil.pw.edu.pl

Abstract

The most important task in tests of resistance of aircraft structures to the terrorist threats is to determine the sensitivity of thin-walled structures to the blast wave load. For obvious reasons, full-scale experimental investigations are carried out exceptionally. In such cases numerical analyses are very important. They allow tuning model parameters for proper correlation with experimental data. With this preliminary analysis experiment can be planned properly. The paper presents a summary of the results of numerical analysis of model of medium size fuselage. Various manufacturing techniques are considered – the skin made of aluminum alloy (2024-T3) and the skins made of modern layered materials (GLARE) were compared. Characteristics of the materials used in FE simulations were obtained experimentally. Modelling of C4 detonation was also discussed. Studies have shown very strong sensitivity of the results to chosen numerical models of materials, formulations of elements, assumed parameters etc. Studies confirm also very strong necessity of the correlation of analysis results with experimental data. Without such a correlation it is difficult to talk about the validation of the results obtained from the “explicit” codes.

Keywords: thin-walled structures, blast wave load, fluid-structure interaction, LS-Dyna

1. Introduction

Due to the growing threat of terrorist attacks some experimental work (e.g. [1]) and numerical analysis have been performed to study the dynamic behaviour of a fuselage subjected to blast pressure loads. The most of experimental data are not accessible to the open research community, therefore numerical modelling of aircraft explosions plays so important role. Some of these finite element (FE) simulations have attempted to predict (simultaneously) the blast wave propagation and related structural damage [2-4]. Other numerical investigations concentrate mainly on structural damage, e.g. [5].

In the paper a numerical analysis of the explosion of C4 in a medium passenger airplane is discussed. In order to investigate the dynamic behaviour of a fuselage, numerical simulations with the commercial explicit FE code LS-Dyna V971 were used.

The airplane structure is loaded by the pressure generated by the explosion of C4 explosive charge of mass 100 g.

Two locations of the charge relative to the fuselage structural members were chosen:

- between two frames (the blast wave will focus on the skin area between two frame beams). For this case three locations are discussed:
 - 20 cm from the floor and 20 cm from the aluminum skin (Load Case 1),
 - 20 cm from the floor and 20 cm from the glare skin (Load Case 2),
 - 50 cm from the floor and 20 cm from the aluminum skin (Load Case 3),
- opposite to a frame (the blast wave will focus directly on a frame beam). For this case one location is discussed:
 - 20 cm from the floor and 20 cm from the aluminum skin (Load Case 4).

Simulation of the blast was performed using the Arbitrary Lagrangian-Eulerian (ALE) formulation. Fluid-structure interaction was performed using a dedicated coupling algorithm with an option that allows erosion of Lagrangian elements.

2. FE modelling

2.1. Geometry

The FE model represents a simplified section of a medium airplane fuselage (Fig. 1.). The airplane structure is meshed with quad elements using *Belytschko-Leviathan shell* formulation.

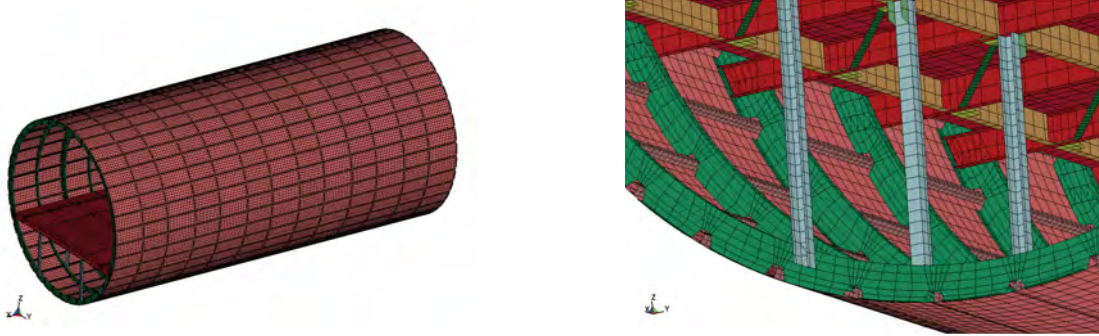


Fig. 1. FE model of fuselage

2.2. Material properties

The airplane structure (excluding skin in Load Case 2, floor and bolts) is made of aluminum alloy (2024-T3). In Load Case 2 the skin is made of GLARE 3 3/2 0.4.

The required material constants for AL2024-T3 are as follows:

- AL2024-T3 (material model: mat_024 – The stress strain behaviour may be treated by a bilinear stress strain curve or a curve of effective stress vs. effective plastic strain. The first value of the effective plastic strain must be zero corresponding to the initial yield stress [6].):
 - mass density (kg/m^3): $\rho = 2923$,
 - Young's modulus (GPa): $E = 68.7$,
 - Poisson's ratio: $\nu = 0.35$,
 - plastic strain to failure: 20%,
 - Fig. 2. describes behaviour of the material (in plastic range).

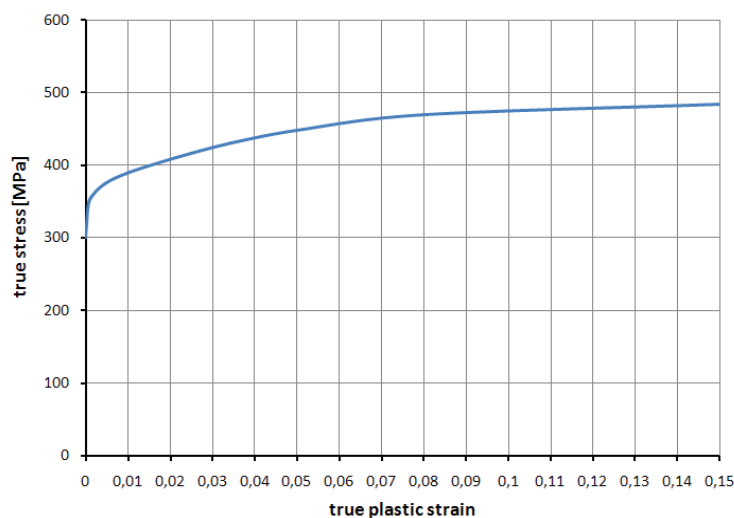


Fig. 2. AL2024-T3 stress-strain characteristic [5]

The floor has a sandwich structure. It is composed of four GFRP layers (glass fibre reinforced polymer) and a Nomex honeycomb core (Fig. 3.).

The required material constants for GFRP and Nomex honeycomb are as follows [7]:

- GFRP (orthotropic material model: mat_059a – an elastic-plastic material model, where the strength values in each orthotropy direction, as well as the shear strength, are taken for the yield function [8]):
 - mass density (kg/m^3): $\rho = 2200$,
 - Young's moduli (GPa): $E_{11} = E_{22} = 29.7$, $E_{33} = 8$,
 - shear moduli (GPa): $G_{12} = 5.3$, $G_{23} = G_{31} = 4.5$,
 - Poisson's ratio: $\nu_{12} = 0.17$,
 - longitudinal and transverse compressive strength (MPa): $X_c = Y_c = 549$,
 - longitudinal and transverse tensile strength (MPa): $X_t = Y_t = 367$,
 - shear strength (MPa): $S_c = 97.1$.

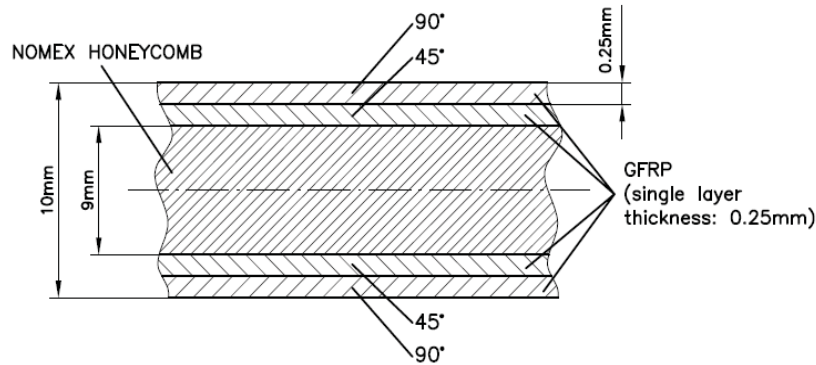


Fig. 3. Floor cross section

- Nomex honeycomb (orthotropic material model: mat_059a):
 - mass density (kg/m^3): $\rho = 49.66$,
 - Young's moduli (Pa): $E_{11} = E_{22} = 69000$, $E_{33} = 33E6$,
 - shear moduli (MPa): $G_{12} = 0.006895$, $G_{13} = 25.511$, $G_{23} = 14.362$,
 - Poisson's ratio: $\nu_{12} = 0.33$.

The lay-up of GLARE (Fig. 4.) is defined as 3 aluminum layers and 4 GFRPP (glass fibre prepreg). The required material constants for GFRPP [5] are as follows:

- GFRPP (orthotropic material model: mat_054 – a composite material model with Chang-Chang failure criterion [6, 8]):
 - mass density (kg/m^3): $\rho = 1800$,
 - Young's moduli (GPa): $E_{11} = 50.6$, $E_{22} = E_{33} = 9.9$,
 - shear moduli (GPa): $G_{12} = G_{23} = G_{31} = 6$,
 - Poisson's ratio: $\nu_{21} = 0.063$,
 - longitudinal tensile strength (MPa): $X_t = 1700$,
 - longitudinal compressive strength (MPa): $X_c = 786.6$,
 - transverse tensile strength (MPa): $Y_t = 191.1$,
 - transverse compressive strength (MPa): $Y_c = 191.1$,
 - shear strength (MPa): $S_c = 53.82$.

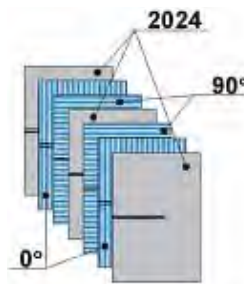


Fig. 4. GLARE lay-up (0° means the hoop direction of the skin)

2.3. Boundary conditions

Figure 5. shows fuselage boundary conditions. All DOFs of nodes at the right end of fuselage (skin and floor) are constrained.

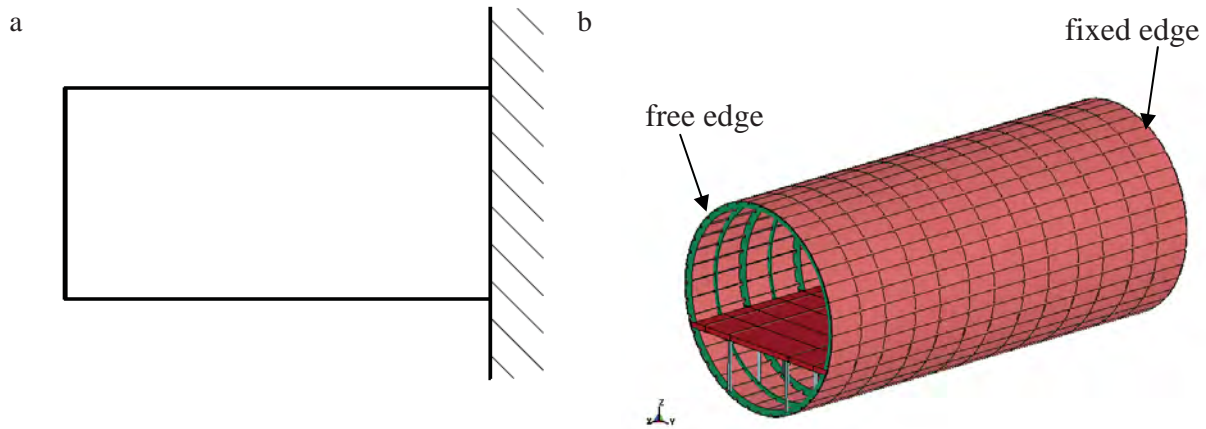


Fig. 5. Constraints

2.4. The Euler domain

The Euler domain (C4 and air) is modelled by ca. 860000 hexa elements with formulation *1 point ALE multi-material element* (Fig. 6.).



Fig. 6. Euler domain

At the free surfaces of the Euler mesh the pressure of 1 bar is applied in order to ensure that the analyzed thermodynamic system will, after the explosion, return to an equilibrium state.

The numerical model used also:

- the linear polynomial equation of state (1) as an EOS describing behaviour of the air

$$p = C_0 + C_1\mu + C_2\mu^2 + C_3\mu^3 + (C_4 + C_5\mu + C_6\mu^2)E, \quad (1)$$

$$\mu = \rho/\rho_0 - 1,$$

p - pressure [Pa],

C_i - polynomial equation coefficients,

E - internal energy per unit reference specific volume [J/m^3],

ρ - mass density [kg/m^3],

ρ_0 - initial mass density [kg/m^3].

- the linear polynomial equation of state coefficients:

$$C_0 = C_1 = C_2 = C_3 = C_6 = 0; C_4 = C_5 = 0.4,$$

- the air properties [2]:
 - mass density (kg/m³): $\rho = 1.129$,
 - pressure (MPa): $p_0 = 0.1$,
 - initial internal energy per unit reference specific volume (kJ/m³): $E = 250$.
- the JWL equation of state (2) as an EOS describing the burning process of C4:

$$p = A \left(1 - \frac{\omega}{R_1 V} \right) \exp(-R_1 V) + B \left(1 - \frac{\omega}{R_2 V} \right) \exp(-R_2 V) + \frac{\omega E}{V}, \quad (2)$$

A, B, R₁, R₂, ω - constants,

p - pressure [Pa],

E - internal energy per unit reference specific volume [J/m³],

V - relative volume [-].

- the JWL equation of state constants [9]:

$$\mathbf{A} = 609.77 \text{ GPa}, \mathbf{B} = 12.95 \text{ GPa}, \mathbf{R}_1 = 4.5, \mathbf{R}_2 = 1.4, \mathbf{\omega} = 0.25,$$

- the explosive properties [2, 9]:
 - mass density (kg/m³): $\rho = 1601$,
 - detonation velocity (m/s): $D = 8193$,
 - initial internal energy per unit reference specific volume (GJ/m³): $E = 9$,
 - Chapman-Jouguet pressure (GPa): $p_{CJ} = 28$.

3. Results – deformation

The deformation of the fuselage subjected to explosion of relatively small charge shows no perforation of the skin, but severe damage of structural members of the reinforcing system occur. In Load Cases 1-3 the blast wave reaches the skin first. The skin deflects what causes break of skin-stiffener and skin-frame connections (titanium bolts). Next, unattached parts of stringers and frame beams start deforming. Plastic strains in this part reach a critical value (20%). Two frame beams, between which the explosive charge was placed, break in their weakest point – in a mousehole area. Nearby stringers are also destroyed.

There are no big qualitative differences between damage of the fuselage model with the aluminum skin (Fig. 7.) and the model with the GLARE skin (Fig. 9.).

In the last case the blast wave focuses directly on a frame beam. As a result of exceeding the plastic strain critical value the loaded beam is destroyed at the height of C4 explosive charge (Fig. 13.).

In all considered Load Cases the floor below the explosive charge was destroyed.

Fuselage deformation obtained from the numerical analysis is shown in Fig. 7-14.

- Load Case 1: between frames; 20 cm from the floor; 20 cm from the aluminum skin:

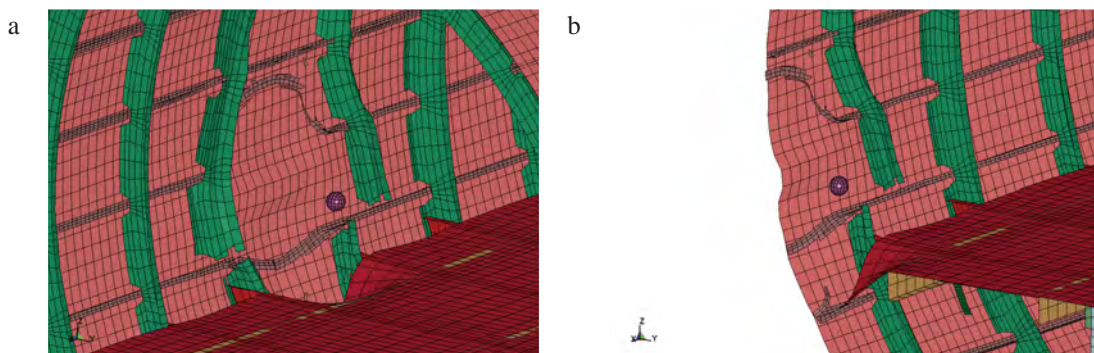


Fig. 7. Model deformation (LC 1; $t = 10 \text{ ms}$)

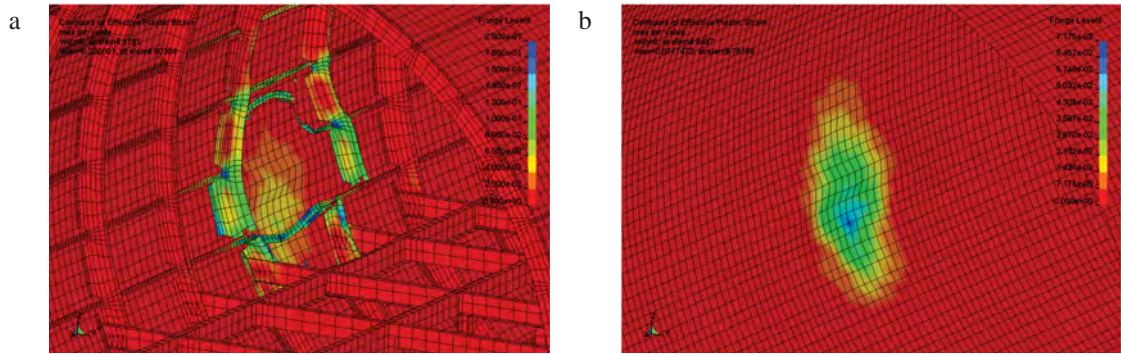


Fig. 8. Plastic strain (LC 1; $t = 10$ ms): a) aluminum structure; b) skin (max 7.2%)

- Load Case 2: between frames; 20 cm from the floor; 20 cm from the glare skin:

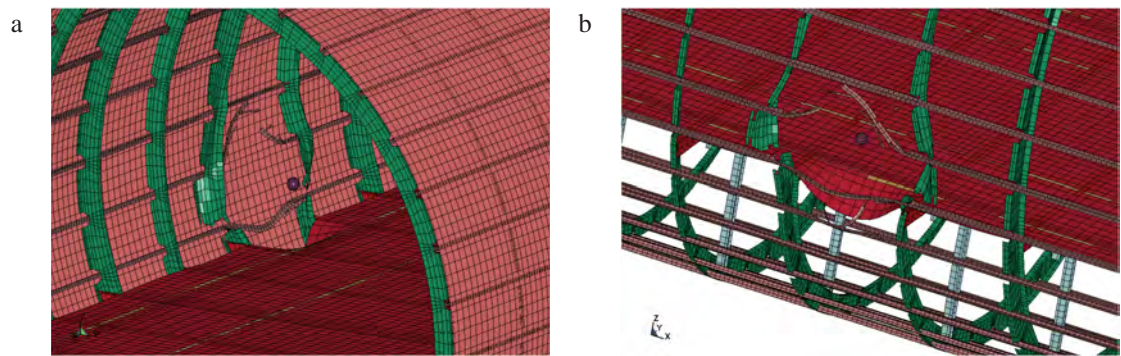


Fig. 9. Model deformation (LC 2; $t = 10$ ms)

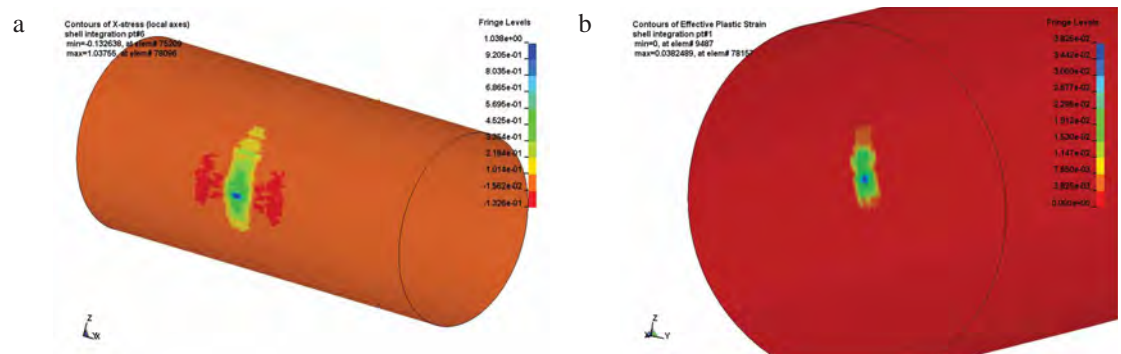


Fig. 10. a) Hoop stresses in one of the prepreg layers ($t = 0.8$ ms); b) plastic strain in outermost skin layer ($t = 10$ ms; max = 3.8%)

- Load Case 3: between frames; 50 cm from the floor; 20 cm from the aluminum skin:

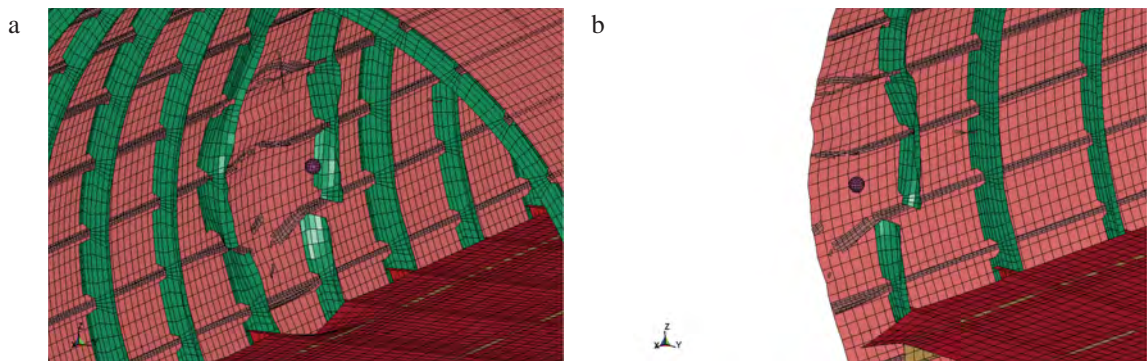


Fig. 11. Model deformation (LC 3; $t = 10$ ms)

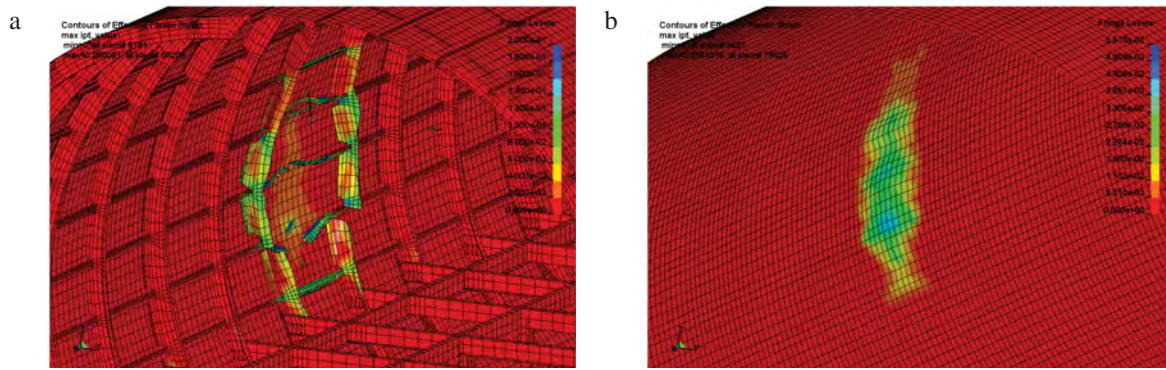


Fig. 12. Plastic strain (LC 3; $t = 10$ ms): a) aluminum structure; b) skin (max = 5.5%)

- Load Case 4: opposite to a frame; 20 cm from the floor; 20 cm from the aluminum skin:

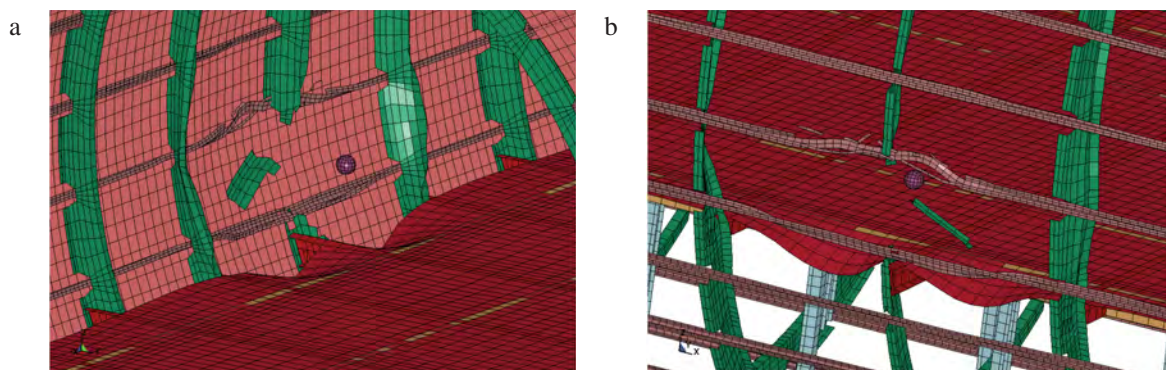


Fig. 13. Model deformation (LC 4; $t = 10$ ms)

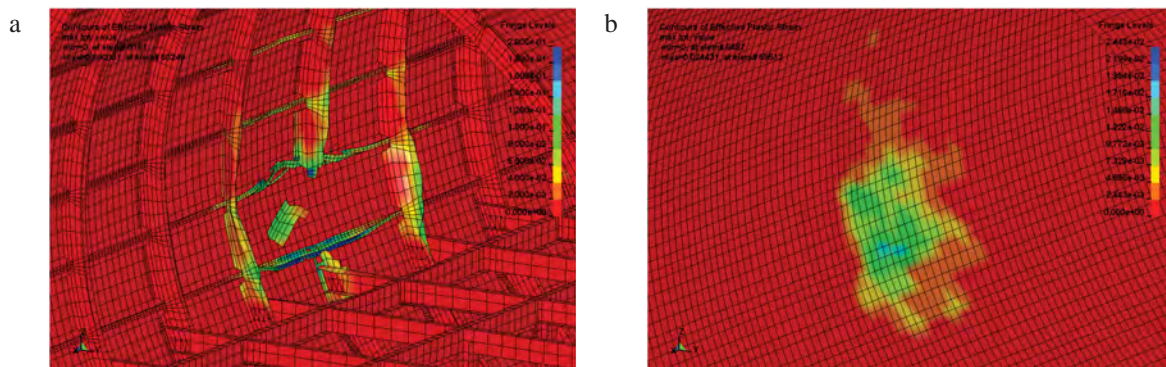


Fig. 14. Plastic strain (LC 4; $t = 10$ ms): a) aluminum structure; b) skin (max = 2.4%)

4. Displacements – time/history

Resultant displacement history plot of representative node (for all considered Load Cases), located (in Load Case 1 and 2) on the skin, opposite to the explosive charge (Fig. 15.), is presented in Fig. 16.

When the blast wave reaches the skin it is set into oscillation. Character of the first phase of the resultant displacement graphs for node 81582 is similar for all considered cases.

Because the skin made of GLARE (Load Case 2) is stiffer than the skin made of aluminum alloy (Load Case 1), it deflects less despite the same pressure load.

Lower value of skin displacement in the last case result from the fact that the blast wave focuses directly on a frame beam first and later on the skin.

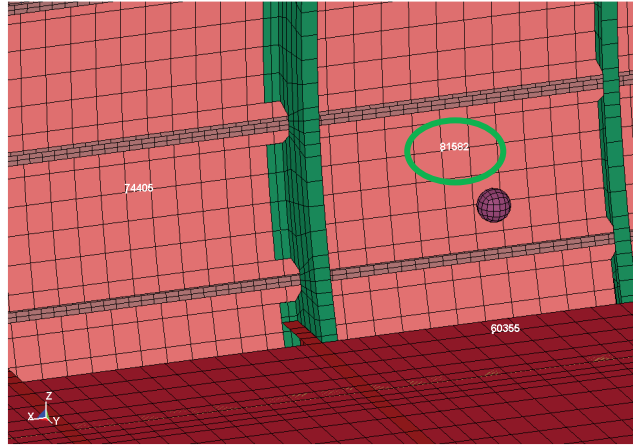


Fig. 15. History node location

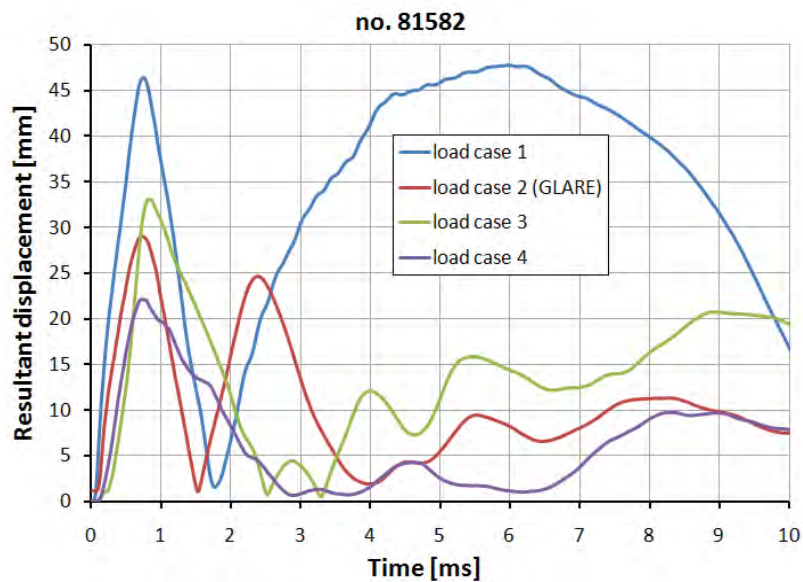


Fig. 16. Resultant displacement (modulus) of node 81582

5. Conclusions

Studies, not discussed here in detail, have shown very strong sensitivity of the results to the numerical models of materials, formulations of elements etc. Studies confirm also very strong necessity of the correlation of analysis results with experimental data, if available. Without such a correlation it is difficult to talk about the correctness of the results obtained from the “explicit” codes. The material libraries of commercial codes are extremely rich now. The same concerns very “elastic” formulation of element models, which results in number of parameters to set (or to choose from). Variations of these parameters results in wide-spread scatter of obtained results, all of them correct from formal point of view.

References

- [1] Wentzel, C. M., van de Kastele, R. M., Soetens, F., *Investigation of Vulnerability of Aircraft Structure and Materials Towards Cabin Explosions*, First International Conference on Damage Tolerance of Aircraft Structures, Delft 2007.
- [2] Kotzakolios, T., *Blast response of flat panels*, EU Project VULCAN: AST5-CT-2006-031011, VULCAN Deliverable D2.1, Patras 2007.

- [3] Moon, Y., Bharatram, G., Schimmels, S., Venkayya, V., *Vulnerability and Survivability Analysis of Aircraft Fuselage Subjected to Internal Detonations* , MSC World Users' Conference, 1995.
- [4] Ashley, S., *Safety in the sky: Designing bomb-resistant baggage containers* , Mechanical Engineering, June 1992, pp. 81-84.
- [5] Soutis, C., *Computational Simulation of blast effects on flat panels* , EU Project VULCAN: AST5-CT-2006-031011, VULCAN 24m Meeting, Barcelona 2008.
- [6] LS-Dyna V971, Livermore Software Technology Corporation, Livermore 2006.
- [7] Cieśla, P., Krzemień-Ojak, P., *Flight pre-stress loading of scaled fuselage* , EU Project VULCAN: AST5-CT-2006-031011, VULCAN Deliverable D3.1, Warszawa 2008.
- [8] Schweizerhof, K., Weimar, K., Münz, Th., Rotter, Th., *Crashworthiness Analysis with Enhanced Composite Material Models in LS-DYNA – Merits and Limits*, LS-DYNA World Conference, Detroit, Michigan 1998.
- [9] Włodarczyk, E., *Wstęp do mechaniki wybuchu*, PWN, Warszawa 1994.